Genomic and Functional Characterization of *Priestia megaterium* MOD5IV isolated from the rhizosphere of *Caesalina spinosa* (Mol.): Enhancing Phytoremediation Potential in Multi-Metal Contaminated Soils

Luis Pouchucq[1*], Andrés E. Marcoleta[2], Carolina Rojas[1], Héctor Arce[1], Cristian Becerra[1], Carola Bahamondes[1], Pablo Lobos-Ruiz[3]

1. Laboratorio de Biotecnología Vegetal y Ambiental, Departamento de Biotecnología, Universidad Tecnológica Metropolitana.
2. Grupo de Microbiología Integrativa, Facultad de Ciencias, Universidad de Chile.
3. División de Innovación, Duna Soluciones Biotecnológicas SpA.

* lpouchucq@utem.cl

ABSTRACT. Heavy metal contamination poses a global threat due to its widespread occurrence and the high toxicity of these elements. Among various methods, phytoremediation has emerged as a preferred approach for the bioremediation of heavy metal-contaminated soils. The search for microorganisms facilitating phytoremediation has become critical to advance ecosystem remediation efforts. Plant growth-promoting bacteria (PGPB) have garnered significant attention in recent decades. In this context, the strain MOD5IV was isolated from the rhizosphere of a *Caesalpinia spinosa* plant thriving on mining waste in Andacollo, Chile. This strain was initially selected for its plant growth-promoting properties.

This study comprehensively analyzed this strain's functional and genomic characteristics. MOD5IV exhibited notable PGPB features, including phosphate and potassium solubilization, nitrogen fixation, phytohormone production, and growth promotion of *Arabidopsis thaliana*. Genomic analysis revealed a chromosome size of 5,254,635 bp and nine distinct plasmids hosting over six thousand genes. Phylogenetic analysis classified the strain within the species *Priestia megaterium*. Functional annotation identified 16 genes associated with tolerance to metals and metalloids, including arsenic (*arsB*/*arsC*) and copper (*copC*/*copD*), as well as genes conferring resistance to cadmium, lead, mercury, zinc, and cobalt. Accordingly, this strain exhibited robust tolerance to multiple metals, notably copper, arsenic, chromium, cadmium, and lead. Regarding its PGPB capabilities, MOD5IV possesses genes related to siderophore production, nutrient solubilization, IAA synthesis, and nitrogen fixation. Furthermore, MOD5IV promotes the growth of *C. spinosa* grown on tailings in laboratory experiments, increasing its capacity to accumulate copper. Overall, *Priestia megaterium* MOD5IV exhibits promising traits for microbe-assisted phytoremediation of metal-contaminated soils.

I**MPORTANCE.** This study explored native metal multi-resistant bacteria for bioremediation of contaminated soils, supporting the phytoremediation perspective. We characterized a novel rhizospheric Priestia megaterium strain at both functional and genomic levels. This strain was isolated from mine waste material in a locality within the arid regions of South America—a geographical area not previously reported for this taxon. These findings may provide new insights into the biogeographical distribution of P. megaterium and its associated genetic determinants. Additionally, the study underlines the strain’s diverse metabolic capabilities, reinforcing its suitability as a model for developing microbe-assisted phytoremediation processes of metal-contaminated soils, increasing the evidence of the Atacama desert as source of microbiological solutions for climate adaptation and environmental remediation.

KEYWORDS. Plant growth promotion; Arsenic resistance; Copper resistance; Contaminated soils, Indole-acetic acid production.

INTRODUCTION

Soil contamination by heavy metals is a significant concern for governments worldwide. Various regulations establish concentration limits for several heavy metals based on land use (Sánchez-Castro et al., 2023; Parviainen et al., 2022). Additionally, regulations require polluting companies, such as those in the mining industry, to take actions to prevent pollution or to remediate contaminated sites. Governments are making concerted efforts to address soil contamination by heavy metals and mitigate its effects on human health and ecosystems (Liu et al., 2021). There are various strategies for the remediation of these contaminated soils, most of which are based on physical or mechanical methods such as excavation and landfilling, surface capping, chemical solubilization and stabilization, and soil washing, among others. Furthermore, biological strategies are generally based on microorganism-mediated or plant-mediated bioremediation methodologies (Souza et al., 2020, Azhar et al., 2022). The best efficiencies at the field scale have been reported combining physical and biological strategies (Sánchez-Castro et al., 2023).

Among the biological strategies, plant-mediated bioremediation, called phytoremediation, is a widely accepted approach due to its economic feasibility and eco-friendliness (Jacob et al., 2018). However, many factors, such as high metal concentrations, nutrient deficiency, soil structure, and physicochemical factors like pH and salinity, limit biomass production and, therefore, the phytoremediation efficiency of plants (Alves et al., 2022). Improving the phytoremediation efficiency of plants at higher metal concentrations is a promising approach, that may be achieved by utilizing plant growth-promoting bacteria (PGPB) (Manoj et al., 2020; Simmer and Schnoor, 2022).

PGPB comprise species from a broad number of genera, including free-living bacteria, those that establish specific symbiotic relationships with plants, bacterial endophytes that colonize plant interior tissues, and cyanobacteria (blue-green algae) (Alves et al., 2022). These bacteria can fix nitrogen, solubilize phosphate and potassium, and produce phytohormones, significantly reducing the need for chemical fertilizers and modulating the effects of environmental stress and pathogen control (Glick, 2012; Romero-Estonllo et al., 2023; Asad et al., 2018; Sijilmassi et al., 2020; Khoshru et al. 2020; Backer et al. 2018; Nazari & Smith 2020; Myo et al. 2019; Hernández-Soberano et al. 2020; Naqqash

et al. 2020). Several bacterial strains isolated from the plant rhizosphere have been reported to improve the productivity and health of plants under metal contamination stress, making them a significant component in phytoremediation processes (Kamaruzzaman et al., 2020; Srivastava et al., 2013; Xu et al., 2018; Wu et al., 2019; Liu et al., 2022).

Among them, *Priestia megaterium* (formerly *Bacillus megaterium*) strains have demonstrated notable plant growth-promoting (PGP) properties, including potassium solubilization and nitrate reduction (Wu et al., 2023; Wang et al., 2020). These strains also exhibit bioremediation capabilities for environments contaminated with heavy metals like zinc (Zn) and cadmium (Cd) (Bhatt and Maheshwari, 2020; Wu et al., 2019) and can induce plant resistance to environmental stresses or pathogens (Cui et al., 2023; Wang et al., 2020; Chakraborty et al., 2005; Zhou et al., 2016).

In this study, we report on the functional and genomic characterization of the PGP and multi-metal-resistant strain *P. megaterium* MOD5IV, isolated from the rhizosphere of *Caesalpinia spinosa* (Mol.) plants thriving in a former mine tailing deposit. Additionally, we investigated its capability to promote growth and enhance the phytoremediation performance.

METHODOLOGY

Strain Isolation. Strains were isolated from the rhizosphere of *Caesalpinia spinosa* plants growing on former tailings from artisanal copper mining near Andacollo, a traditional mining city located in Elqui Province in northern Chile (30°15.381’S 71°04.551’W). Soil samples (1 g) collected from the mine tailings were added to 10 mL of sterile water and vortexed vigorously for 1 min. Serial tenfold dilutions were prepared and then spread on Soy Trypticase Agar (TSA) medium (Difco®). Plates were incubated at 28°C for 24 h.

Basic qualitative PGPB analysis. Nitrogen fixation was determined by growth on Ashby-agar medium (0.2 g/L KH_2PO_4, 0.2 g/L $MgSO_4$, 0.2 g/L NaCl, 0.2 g/L $CaSO_4$, 5.0 g/L $CaCO_3$, 5.0 g/L sucrose, 5.0 g/L glucose, and 15 g/L agar) (Becking, 2006). Phosphate and potassium solubilization index were determined cording Sijilmassi (2020), using Pikovskaya agar medium (10.0 g/L glucose, 0.2 g/L NaCl, 0.002 g/L $FeSO_4$, 0.002 g/L $MnSO_4$, 0.2 g/L KCl, 0.1 g/L $MgSO_4$, 0.5 g/L $(NH_4)_2SO_4$, 0.5 g/L yeast extract, 5.0 g/L $Ca_3(PO4)_2$, and 15 g/L agar) and modified Pikovskaya agar medium (10.0 g/L glucose, 0.2 g/L NaCl, 0.002 g/L $FeSO_4$, 0.002 g/L $MnSO_4$, 0.2 g/L KCl, 0.1 g/L $MgSO_4$, 0.5 g/L $(NH_4)_2SO_4$, 0.5 g/L yeast extract, 5.0 g/L KNO_3, and 15 g/L agar), respectively. Siderophore production

was tested using the chrome azurol S method in solid medium (CAS-agar), as described by Alexander and Zuberer (1991). The bacterial cultures were incubated at 28°C for 24 h. Orange halos around the colonies indicated siderophore production.

IAA production was determined colorimetrically, according to Glickmann and Dessaux (1995). The isolates were inoculated in Soy Trypticase Broth (TSB) medium with and without tryptophan (500 µg/ml) and incubated at 28°C for 4 days with shaking at 250 rpm. A 1 mL aliquot was removed from each tube and centrifuged at 10,000 rpm for 10 min. 200 µL of the supernatant from each sample was transferred to a 96-well microplate, to which 50 µL of Salkowski reagent (12 g/L $FeCl_3$ and 7.9 M H_2SO_4) were added. The mixture was incubated at room temperature for 30 min, and the absorbance was measured at 530 nm using a microplate spectrophotometer (EPOCH-II BioTek). The IAA concentration in the culture was determined using a calibration curve of pure IAA (Supelco®) as a standard, following linear regression analysis.

Phosphate uptake quantification. PO_4 was quantitatively determined using the Mo-Blue Method (Watanabe & Olsen, 1965; Nautiyal, 1999). A pre-culture was incubated in 10 mL of TSA medium overnight at 29°C with agitation (150 rpm). The following day, the culture was adjusted to 10^8 CFU/mL, and 100 µL were inoculated into 10 mL of PKV medium. The cultures in PKV medium were incubated at 29°C with constant agitation (150 rpm) for 72 h. One milliliter of the culture was clarified by centrifugation (12,000 x g), and 250 µL of the supernatant were placed in a microcentrifuge tube and digested by adding concentrated sulfuric acid in a 1:1 v/v ratio. 200 µL of the digested samples were placed in triplicate in a 96-well microplate. 100 µL of Mo-Blue reagent was added to each sample and mixed gently by pipetting. Absorbance was recorded using a microplate spectrophotometer (EPOCH-II BioTek) set at 820 nm. A calibration curve was constructed with a PO_4 standard (KH_2PO_4, Certipur®, Supelco).

***Arabidopsis thaliana* growth promotion.** *A. thaliana* (Col-0) seeds were treated with 2% Tween 20 for 10 min with gentle agitation. The seeds were then rinsed thrice with sterile distilled water. Afterward, the seeds were soaked in 70% ethanol for 30 s and rinsed three times with sterile distilled water. Subsequently, the seeds were dipped in 1% sodium hypochlorite for 10 min and finally rinsed with sterile distilled water five times. Seeding was carried out in polycarbonate Petri plates with Murashige & Skoog (MS) medium supplemented with sucrose (10 g/L) and agar (8 g/L) at pH 5.7. Three seeds were placed into each plate at 2 cm from each other and incubated at 4°C for 48 h for

stratification. After the stratification period, the plates were placed vertically (at a 65° angle) in an incubator with a photoperiod of 16:8 h (light:dark) at 24°C for 6 days. On the sixth day of culture, 20 µL of MOD5IV at 10^8 CFU/mL were inoculated 2 cm from the seedling roots. The seedlings were incubated for an additional 8 days under the same conditions. Finally, the length of the primary root, number of secondary roots, rosette diameter, leaf area, and number of true leaves were measured. This assay was carried out in triplicate, with a total of 9 plants for each isolate.

IAA quantification by HPLC. MOD5IV (0.3 mL of 10^8 CFU/mL culture) was inoculated into 30 mL of TSB medium, with and without tryptophan (500 µg/mL), in 50 mL centrifuge tubes, and incubated at 28°C for 72 h with shaking at 250 rpm. After incubation, the culture was centrifuged at 7,000 rpm for 10 min for cell clarification. 25 mL of the supernatant were adjusted to pH 2.5 with HCl. IAA was extracted with ethyl acetate in a 1:3 ratio, vortexing for 1 min. The ethyl acetate was evaporated at 40°C overnight, and the resultant powder was dissolved in 3 mL of methanol. The sample was analyzed by HPLC (Ultimate 3000 Thermo®) using a pre-equilibrated reverse-phase column (C18 LiChrosphere 5 µm, Merck®) under isocratic conditions with a mobile phase of water:acetonitrile: acetic acid (85:15:1). The chromatograms were run at a flow rate of 1 mL/min at 20°C. Detection was performed by UV light absorption at 252 nm. A calibration curve was constructed using an HPLC-grade standard of IAA (Supelco®) (Shao et al, 2015, Tien et al, 1979).

Quantification of ammonia production. Nitrogen fixation was determined based on ammonia production using the Nessler's method (Kamaruzzaman et al, 2020 and, Wu et al, 2019). MOD5IV preinoculum was prepared in TSB and incubated overnight at 29°C with shaking at 150 rpm. The next day, CFUs were determined using the microdroplet technique. Inocula were prepared in triplicate tubes with 20 mL of peptone water (20 g/L peptone and 30 g/L NaCl). The tubes were incubated at 29°C for 5 days with shaking at 150 rpm. After incubation, CFU was determined using the microdroplet technique. Bacterial cells were eliminated by centrifugation at 12,000 rpm for 10 min. Then, 200 µL of the culture supernatant was transferred to new microcentrifuge tubes. Subsequently, 1 mL of Nessler's reagent was added. The optical density was measured at 450 nm using a sterile 96-well microplate. A calibration curve was generated using an ammonium standard (NH_4Cl Certipur® Supelco) on the same plate.

Metal exposure and MIC determination. The strain was inoculated from a previous culture adjusted at 10^8 CFU/mL in a proportion of 1:100 in TSB medium supplemented with previously diluted gradient of metal concentrations: copper ($CuSO_4$), mercury ($HgCl_2$), chromium ($K_2Cr_2O_7$), lead

($Pb(C_2H_3O_2)_2$), cadmium ($CdCl_2$) and arsenic (As_2O_3) (ReagentPlus®, Sigma-Aldrich). pH was adjusted to 7.5. The cultures were placed in triplicate into a sterile 96-well microplate and incubated at 28°C with agitation of 200 rpm into an Epoch-II (BioTeck) microplate reader. Cell proliferation was determined by absorbance at 600 nm, measuring every 0.5 h for 24 h. The minimum inhibitory concentration (MIC) was determined for each metal as the concentration needed to avoid culture growth in the conditions previously mentioned.

Promotion of *C. spinosa* Growth in Metal-Contaminated Substrate. *C. spinosa* seeds were treated with concentrated sulfuric acid for 45 min. The solution was then neutralized with sodium bicarbonate. The seeds were rinsed with distilled water and placed into plastic containers containing 80 g of contaminated soil from the same mine tailing where the MOD5IV strain was collected, amended in a 50:50 ratio with sterilized plant substrate based on Sphagnum sp. H2–H4 von Post (Kekkila® Professional substrate). The MOD5IV inoculum was grown overnight in TSB medium, and the cell density was adjusted to 10^8 CFU/mL. One milliliter of this inoculum was added to each substrate container. Control containers received TSB medium without bacteria. One seed was placed in each container, and the containers were incubated at 28°C for 60 days with a 16:8 light-dark photoperiod. Five replicates were prepared for each condition.

After the culture period, seedlings were carefully extracted and rinsed with distilled water. Growth parameters, including root length and dry mass, were recorded. The dried tissues were used to determine copper (Cu) concentration. The plant material was calcined in a muffle furnace until white ash was obtained. The white ash was suspended in nitric acid and diluted with distilled water (1:10). The solutions were clarified by filtering, and Cu concentrations were quantified by atomic absorption spectroscopy using an AAnalyst™ 700, PerkinElmer instrument. Metal concentrations in the substrate were quantified by X-ray fluorescence (XRF). A soil (tailing) sample was collected during bacterial isolation, from a 1 m × 1 m area to a depth of 15 cm using a shovel. The amount of soil was then reduced using the quartering method (ASTM International, 2018) to a representative 1 kg sample. The tailing material, both alone and amended, was dried in an oven at 60°C until no mass loss was observed. The samples were analyzed using X-ray fluorescence (XRF) with an S1 Titan 600 Handheld XRF Analyzer (Bruker)

Genomic sequencing, assembly and annotation. Genomic DNA was purified from an overnight culture of the MOD5IV strain grown in TSA, using the genomic extraction kit Wizard (Promega®) following the manufacturer's recommendations. Genomic DNA was sequenced by Illumina® and

Nanopore® platforms. Illumina sequencing (100-pb paired-end reads) was performed through the TruSeq Nano DNA Kit for library preparation and run in a XLEAP-SBS machine (Illumina SBS technology). The obtained reads (15,374,518) were quality-checked by the FastQC 0.11.9 software (Andrews, S., 2010). The Nanopore sequencing library was prepared using the Ligation Sequencing kit LSK-110, following the manufacturer's guidelines. 5–50 fmol of the library were loaded into a FLO-MIN106D flow cell and sequenced using a MinION device (Nanopore Technologies Ltd., Oxford, UK). The quality and length of the Nanopore reads were assessed by Nanoplot from the Nanopack toolkit (Oxford Nanopore). Unicycler 0.4.9b (Wick et al 2017) was used in hybrid mode for genome assembly. Gene annotation was performed using the Rapid Annotation program by the Subsystem Technology (RAST) server (Overbeek et al. 2014). Additional functional annotation was carried out using the KEGG (https://www.kegg.jp/kegg/kegg2.html) database. The Resistance Gene Identifier (RGI) and the CARD database (https://card.mcmaster.ca/analyze/rgi) (Alcock et al. 2020) were used for resistome prediction.

RESULTS

Isolation and initial characterization. To screen for the presence of metal-resistant bacteria with high-efficiency plant growth promotion (PGP) properties, the rhizosphere soil of *Caesalpinia spinosa* was selected because it was thriving on a former mine tailing deposit with high concentrations of metals (Supplementary Table 1). The isolation of pure strains was performed on copiotrophic TSA medium agar plates. A series of bacterial strains were obtained and screened for PGP properties including nitrogen fixation, phosphate and potassium solubilization, IAA production, and promotion of *Arabidopsis thaliana* growth. The bacterial isolates that most effectively induced the growth of *A. thaliana* are shown in Figure 1A. Of these, the MOD5IV isolate exhibited the greatest induction of primary root growth.

The MOD5IV isolate formed white colonies with lobulated margins on TSA medium and showed a bacillar Gram-positive morphology under microscopic analysis (Figure 1B), with a cell length of 10.5 ± 2.4 µm. To confirm the taxonomic position of MOD5IV, we sequenced the 16S rDNA (Accession number MN744240.1). BLAST analysis indicated the highest similarity with *Priestia megaterium* SR01-1 and *Priestia megaterium* DK2 (100% identity for both). The species distribution map of the 16S rDNA gene compared to the 16S rRNA database is shown in Figure 1C, where more than 80% of the hits obtained corresponded to sequences annotated as belonging to the taxa *Priestia megaterium* (NCBI: txid1404). This evidence, combined with the comparison results of 16S rDNA gene sequence-

based and whole-genome sequence-based phylogenetic trees elaborated with TYGS (Meier-Kolthoff et al, 2022) (Supplementary Figure 1), allowed us to conclude that MOD5IV belongs to the *Priestia megaterium* species. This represents the first reported complete genome sequence of the taxa (*P. megaterium*) for this geographic location (Adeniji et al. 2025).

MOD5IV Plant Growth Promotion Properties. The basic plant-growth-promoting properties of MOD5IV were examined (Figure 1D). MOD5IV was able to solubilize phosphate and potassium in solid PKV agar medium. The solubilization indexes for both nutrients were 8.6 and 35.3, respectively, after 72 h of culture. PO_4 solubilization was also quantified using the Mo-Blue method, determining that MOD5IV was capable of incorporating 69 ± 8 µg(PO_4)/mL directly from inorganic $Ca_3(PO_4)_2$ present in the PKV medium during 72 h of culture. Similarly, MOD5IV was able to grow in nitrogen-deficient Ashby medium, indicating the presence of a nitrogen fixation mechanism. Quantification of NH_4 production through the Nessler reaction indicated that MOD5IV produced 100.6 ± 3.6 µgNH4/mL in a 5-day culture. Siderophore production was evidenced by the formation of a characteristic halo on CAS-agar medium. The production of the phytohormone IAA was assessed colorimetrically using the Salkowski method and also by HPLC analysis. In a 72-h culture, the MOD5IV strain produced 40.9 µg/mL of IAA, according to the Salkowski method, and 0.3 µg/mL of IAA using HPLC analysis. This difference of two orders of magnitude between the methods is due to the Salkowski method reacts positively with various auxins and their precursors. In contrast, the HPLC method can differentiate between different types of auxins and precursors as indole-3-lactic acid (ILA), tryptamine, indole-pyruvic acid, among others (Guardado-Fierros et al, 2024; Tien et al, 1979).

The plant growth-promoting properties (PGPR) of MOD5IV were tested using a co-culture method with *Arabidopsis thaliana* in solid plant MS medium. Results shown in Figure 2 indicate that the presence of MOD5IV induced a significant increase in all of the growth parameters tested: length of the primary root (Figure 2A), number of secondary roots (Figure 2B), and rosette diameter (Figure 2C). The increase was even more pronounced in the parameters related to the root. Representative images are shown in Figure 2D.

MOD5IV genomic features. To gain deeper insights regarding the genetic properties of the MOD5IV strain, we performed complete genome sequencing using Illumina and Nanopore sequencing platforms. 2,321,552,218 bp of raw Illumina data were obtained, corresponding to 15,374,518 100-bp reads. No quality filtering was required since the FasQC analysis indicated no overrepresented sequences and a quality Phred score above 30 throughout all the reads. The Nanopore platform generated 575,784,902

bp (56,256 reads, N50=32,731 bp). The complete genome was assembled using a hybrid approach, taking advantage of the higher-accuracy short reads from the Illumina platform and the significantly longer Nanopore reads.

The MOD5IV genome showed a total size of 5.69 Mb with an average GC content of 37.73%, consisting of a 5.25 Mbp circular chromosome and 9 plasmids designated pMOD5IV1 to pMOD5IV9 (Table 1, Figure 3A). Taxonomic classification according to the Genome Taxonomy Database confirmed this strain belonging to the *Priestia megaterium* species. A schematic representation of the replicons generated with the CG View server (Wang et al 2020; Stothard and Wishart 2005) is provided in Figure 3A. Genome annotation showed 6,286 protein-coding genes, 75 repeat regions, and 189 RNA genes divided into 143 tRNAs and 46 rRNA (Table 1). The general features of the *P. megaterium* MOD5IV genome were compared with three genomes of *P. megaterium* strains with different numbers of plasmids (NTC-2, DMS319, KF18 and NBRC15305 = ATCC14581) and one *P. flexa* strain genome (KLBMP 4941) (Table 1). Homologous genome alignment drafts (Figure 3B) (Alikhan et al 2011) showed that the MOD5IV chromosome shared the general *Priestia megaterium* genome topology, except for two regions centered at 3 Mbp and 4.6 Mbp, which apparently correspond to insertions due to differences in the GC content. These insertions carried some open reading frames related to DNA repair and protein translation, such as Vsr-endonuclease and Aspartate-tRNA-synthetase. Also, the regions between 1.6 and 1.9 Mbp, around 3 Mbp, and between 3.6 and 3.8 Mbp showed a marked anomaly in the GC content, corresponding to divergent regions among the four strains compared. In these regions it was possible to find genes related to sporulation, metal resistance, multidrug resistance, transcriptional regulators, chaperones and DNA repair. Phage genes were detected only in the region around the coordinate 3.0 Mbp.

MOD5IV Genome Functional Annotation. To obtain better results in genomic annotation, the analysis was complemented using two different databases, RAST and KEGG (Shrestha et al, 2022). The RAST platform annotated and functionally categorized 2,068 from a total of 5,722 coding sequences present in the MOD5IV genome. Of these, 2,025 were found in the chromosome, with the remainder distributed among the different plasmids. A total of 1,361 chromosomal genes (25%) were assigned to 334 subsystems by RAST. The top five categories in strain MOD5IV were “Amino Acids and Derivatives” (414), “Carbohydrates” (318), “Cofactors, Vitamins, Prosthetic Groups, Pigments” (159), “Protein Metabolism” (243), and “Nucleosides and Nucleotides” (108) (Figure 4A). No matches were found for the “Photosynthesis” and “Phages, Prophages, Transposable Elements, Plasmids”

categories. Meanwhile, the KEGG platform identified 6,022 genes, with 2,915 genes annotated and classified into KEGG categories. The top five categories were “Protein Families: Genetic Information Processing” (381), “Carbohydrate Metabolism” (343), “Protein Families: Signaling and Cellular Processes” (324), “Environmental Information Processing” (227), and “Unclassified: Metabolism” (199) (Figure 4B).

The proteome of MOD5IV was extracted from the RAST server and submitted into the FusionBD server (https://services.bromberglab.org/fusiondb/) to search for similarities with related strains. The MOD5IV proteome contained 5449 proteins, which were mapped to 3780 functions. 573 proteins could not be mapped to any function in the BD database. The most similar proteome found in the database was *P. megaterium* DSM319 (TAXID 592022) with 81% similarity and 3511 shared functions.

Core and accessory genomes were determined using the Spine/AGEnt/ClustAGE tool (http://spineagent.fsm.northwestern.edu/index_age.html) and 21 *Priestia megaterium* reference strains (DSM319, YC4-R4, KF18, 207, NCT-2, KNU-01, 5-3, S188, S2, FDU301, BIM B-1314D, NBRC15305 = ATCC14581, BHS1, IGA-FME-1, CDC 2008724142, H2, 2020WEIHUA_L, BP01R2, CK7, F20, and KF18) available in BioProject database with an assembly level of complete genome. Approximately 25.5% of the MOD5IV genome was accessory. The core genome (4,239,675 bp) consisted of 4,581 coding sequences with a GC content of 38.7%. Meanwhile, the accessory genome had 1,783 coding sequences and a GC content of 34.9%. The differences in GC content between the core and accessory genomes could indicate horizontal gene transfer. RAST annotation of the accessory genome revealed that the principal subsystem categories corresponded to “Amino Acids and Derivatives,” “Stress Response,” and “Cell Wall and Capsule.” This differed from the core genome, where the principal categories were “Amino Acids and Derivatives,” “Carbohydrates,” and “Protein Metabolism” (Figure 5). The presence of genes classified into the “Virulence, Disease, and Defense” subsystem also increased considerably in the accessory genome of MOD5IV, including genes related to copper homeostasis, cobalt-zinc-cadmium resistance, and antibiotic resistance. Meanwhile, in the “Stress Response” subsystem, the accessory genome of MOD5IV contained genes related to osmotic stress (choline and betaine uptake), cold shock, and bacterial hemoglobins. A total of 429 coding sequences were present in the nine plasmids of MOD5IV (Table 2). In the best case, RAST annotation covered no more than 14% of the sequences. Among the annotated sequences we found genes related to isoprenoid biosynthesis, sugar ABC transporters, oxidative stress (catalase), osmotic stress (glycine/betaine transporters or choline-binding protein A), and phage capsid genes.

Plant growth promotion and resistance genes. As expected, the MOD5IV genome contained several genes related to both direct and indirect mechanisms of plant growth promotion (Backer et al, 2018). Regarding direct mechanisms, MOD5IV included ten genes related to PO_4 solubilization and uptake, such as *phoU*, *phoP*, *phoR*, *phoB*, and *phoH*; two genes related to potassium uptake, *kefA* and the large-conductance mechanosensitive K channel; 21 genes related to siderophore production and Fe assimilation; and 12 genes related to nitrogen assimilation, including *norD*, *norQ*, nitrate reductase, and glutamine synthase, among others. Concerning indirect plant growth-promoting mechanisms, MOD5IV housed 10 genes related to auxin production (indole-acetic acid, IAA), primarily belonging to the indole-3-pyruvic acid and tryptamine synthesis pathways (Table 3).

The MOD5IV genome showed a variety of metal resistance genes distributed principally into the chromosome. These include arsenic resistance genes grouped into two putative operons: one included *arsC*, *arsB*, and *arsR*, while the other contained only *arsR* and *arsB*. Additionally, copper resistance genes were grouped into three putative operons: one operon encodeded a copper-translocating P-type ATPase, *copD*, and *ycnl*; another contained *copC*, *copD*, and *cutC*; and the third encoded a copper-translocating P-type ATPase, *copZ*, and *csoR*. Cadmium resistance genes *cadA* and *cadC* were grouped into one putative operon. Three mercury-sensitive transcriptional regulator genes (*merR)* were present in the genome not organized into any *mer* operon. Resistance genes for other metals such as lead, cobalt, and zinc were also present and organized in an operon containing the *P-type* Cd^{2+}/Zn^{2+} *transporter*, the transcriptional repressor *czrA*, and the cobalt/zinc/cadmium resistance protein *czcD* (Table 3).

Using the Resistance Gene Identifier (RGI) tool (Alcock et al., 2023), we further characterized the MOD5IV resistome, identifying 12 probable antibiotic resistance genes, which include six genes for glycopeptide antibiotic resistance (*vanY/I/B/W/G/T*), one for tetracycline resistance (*tetQ*), one for cephalosporin resistance *(bcIII*), one for fosfomycin resistance (*fosB*) and three small multidrug resistance efflux pump (*qacG/J*).

MOD5IV metal resistance and phytoremediation potential. Metal exposure experiments were performed to establish the resistance range of MOD5IV. The strain was exposed to increasing concentrations of common contaminating metals diluted in TSB medium, and growth kinetics were monitored by measuring the absorbance at 600 nm. Figure 6 summarizes the resistance level of the MOD5IV strain, which exhibited high tolerance to multiple metals (and metalloids), including arsenic,

chromium, lead, and copper. Conversely, mercury and cadmium-induced toxic effects at low concentrations.

MOD5IV was initially isolated from the rhizosphere of a *C. spinosa* specimen. Accordingly, the same plant species was used to test the capabilities of MOD5IV to promote plant growth and improve phytoremediation potential in conditions of high metal concentrations in the substrate. A co-culture experiment was conducted in which *C. spinosa* seedlings were grown for 60 days in tailings material amended with organic substrate and treated with MOD5IV. After the culture period, the seedlings were extracted, and growth parameters were measured. As could be seen, seedlings inoculated with MOD5IV showed a significant increase in growth parameters in comparison with non-inoculated seedlings, including the length of roots and aerial parts (shoots + leaves) (Figure 7A) and dry weight (Figure 7B) parameters. Additionally, an increase in Cu uptake was recorded (Figure 7C), corresponding to an increase in Cu concentration of approximately 63% in the aerial parts and 29% in the roots. Although *C. spinosa* appears to be very tolerant to conditions of high metal concentrations in the substrate, it is not a hyperaccumulating plant, as the Cu concentration in the roots and aerial parts showed an accumulation of only 3% and 0.6%, respectively, of the copper present in the substrate, which registers 1,974 mg(Cu)/kg.

DISCUSSION

As stated above, the MOD5IV genome contains a complex array of metal resistance genes and operons, conferring resistance to multiple metals, as has been previously reported for other *P. megaterium* strains. For example, the strain HgT21 contains two complete type II *mer* operons in its genome and tolerates about 6.8 mg/L of Hg (Guzmán-Moreno et al., 2022). MOD5IV contains the transcriptional regulator *merR* gene repeated three times in its genome but lacks the rest of the *mer* operon elements. Despite this, MOD5IV could resist 2 mg/L of Hg^{2+} in solution. The HgT21 strain also contains the *ars* operon and tolerates high concentrations of arsenic (5,697.3 mg/L As(V)) in the form of Na_3AsO_4, whereas MOD5IV tolerated over 1,000 mg/L of arsenite (As(III)) (as As_2O_3), which results more toxic than arseniate (As(V)). This high tolerance correlates with the presence of two *ars* operons in its genome. Higher concentrations of As(III) could not be tested due to its low solubility in the culture medium. MOD5IV also resisted the presence of a high concentration of copper in the culture medium (MIC 125 mg(Cu)/L) at a similar range as the *P. megaterium* HgT21 strain (190 mg(Cu)/L). This last relates to the presence of three putative copper operons in its genome, including one *csoR-copZA*

system that has been described to confer resistance to high levels of copper (Efe D. 2020; Smaldone et al., 2007).

Regarding cadmium resistance, MOD5IV contained one *cad* operon and other operons conferring resistance to lead, zinc, cadmium, and cobalt, resulting in a resistance of 8 mg/L of Cd in solution, which is slightly greater than the previously reported Cd-resistant *P. megaterium* BM18 strain that has demonstrated resistance of over 4.5 mg(Cd)/L (Wu et al., 2019). MOD5IV also showed high resistance to Pb with a MIC of 500 mg/L, considerably more than other *P. megaterium* isolates, which have shown a resistance of 20.7 mg/L of Pb in solution (Roane, 1999). However, strains of the genus *Bacillus* have shown resistance to similar amounts of Pb (Abdelkrim et al., 2018). Finally, MOD5IV showed a MIC of 250 mg/L of Cr, despite the absence of specific Cr resistance genes, such as the *chr* operon. Other *P. megaterium* isolates have resisted 150 mg/L of Cr(VI) (Srinath et al, 2002). Notably, MOD5IV resisted more different metals than other reported *P. megaterium* strains.

Several studies have demonstrated the ability of metal-resistant PGPB strains to increase plant growth and phytoremediation potential in metal-contaminated soils (Bhatt and Maheshwari, 2020; Chakraborty et al, 2006; Tirry et al, 2021; Tang et al, 2020; Ustiatik et al, 2021; Ullah et al, 2022; Kong et al, 2015; Gao et al, 2010; Ma et al, 2011), including some belonging to *P. megaterium* taxa as the strain HgT21 (Guzmán-Moreno et al, 2022) and M18-2 (Wu et al 2019). To our knowledge, MOD5IV is the first multi-metal resistant and PGPB *P. megaterium* strain reported with the capacity to increase the phytoremediation potential of copper in contaminated soils.

Plant growth-promoting bacteria can act by reducing the toxic effects of metals or by producing phytohormones (Wu et al 2019). Depending on the PGP traits, different bacteria play a key role in promoting plant development besides reducing the toxicity or damage to plants exposed to stress generated by different heavy metals. Additionally, PGPB strains produce various metabolic compounds such as organic acids, siderophores, EPS, and biosurfactants, which can alter the redox state, chelation, precipitation, and immobilization of the metals in the rhizospheric environment, thereby enhancing the plant phytoremediation efficiency (Manoj et al, 2020; Alves et al, 2022).

Upon searching the MOD5IV genome, we found no genetic determinants for the surfactin synthesis pathway. However, copper resistance genes may be crucial in conferring phytoremediation efficiency to *C. spinosa* plants. Specifically, the *copD* and *copC* genes, which are involved in the import of copper into the cytoplasm (Lawton et al., 2016), and the cytoplasmic copper-binding protein CutC (Latorre et

al., 2011) reduce copper toxicity and facilitate its safe transport within the cell (Rensing & Grass, 2003). Additionally, the phosphate solubilization ability of the tested bacterial strain likely plays an important role in enhancing plant uptake of soil minerals and increasing the uptake of metals in contaminated soils through the secretion of organic acids. Bacteria such as MOD5IV and other metal-tolerant rhizobacteria selected by plants, are crucial for metal detoxification in metalliferous soils. They help plants endure metal toxicity and improve metal uptake (Ma et al., 2015c; Manoj et al., 2020; Mengoni et al., 2001). Thus, the efficiency of phytoextraction can be enhanced by promoting both plant growth and metal bioavailability in the soil (Ashraf et al., 2019).

CONCLUSIONS

The isolation and functional and genomic characterization of rhizospheric bacterias that promote the growth and enhance the resistance of plants growing in metal contaminated soils in the arid regions of South America had led to the identification of the *Priestia megaterium* MOD5IV strain, which was the first complete genome sequence of the taxa (*P. megaterium*) reported from this geographic location (Adeniji et al. 2025), increasing the evidence of the Atacama desert as source of microbiological solutions for climate adaptation and environmental remediation (Castro-Severyn et al. 2024; Astorga-Eló et al. 2021; Maza et al. 2019).

The strain *P. megaterium* MOD5IV, exhibited significant plant growth-promoting features, including mechanisms for enhanced nutrient availability and phytohormone production. Accordingly, the MOD5IV genome includes genes associated with plant growth promotion, such as nitrogen metabolism, phosphate and potassium uptake, phosphate solubilization, synthesis of organic acids, and IAA synthesis. Additionally, genes involved in resistance to multiple heavy metals, such as lead, cadmium, arsenic, mercury, and copper, correlating with high tolerance to these metals. Moreover, in controlled experiments with metal-contaminated substrates, the MOD5IV strain improved the phytoremediation potential of *C. spinosa*, increasing both the plant biomass and the metal uptake. In summary, these results provide valuable genomic and experimental resources for further studies and applications of *P. megaterium* MOD5IV in bioremediation processes, particularly in heavy metal-contaminated soils.

FUNDING. This work was supported by “Funding By “Concurso Interno de Fomento a la I+D+I o Creación” UTEM, LPR21-05, and by the grant FONDECYT 1221193 from Agencia Nacional de Investigación y Desarrollo (ANID, Chile).

AUTHOR CONTRIBUTION. Luis Pouchucq, Conceptualization, Data curation, Formal analysis, Investigation, Methodology, Project administration, Resources, Software, Validation, Visualization, Writing – original draft, Writing – review and editing. **Andrés E Marcoleta**, Data curation, Investigation, Methodology, Project administration, Resources, Software, Validation, Visualization, Writing – original draft, Writing – review and editing. **Carolina Rojas** and **Hector Arce,** Formal analysis, Investigation, Methodology. **Cristian Becerra**, **Carola Bahamondes** and **Pablo Lobos**, Project administration, Resources, Validation, Visualization, Writing – review and editing

ACKNOWLEDGMENTS. We thank Duna Soluciones Biotecnológicas SpA. for providing materials and samples used in this study.

Figure 1

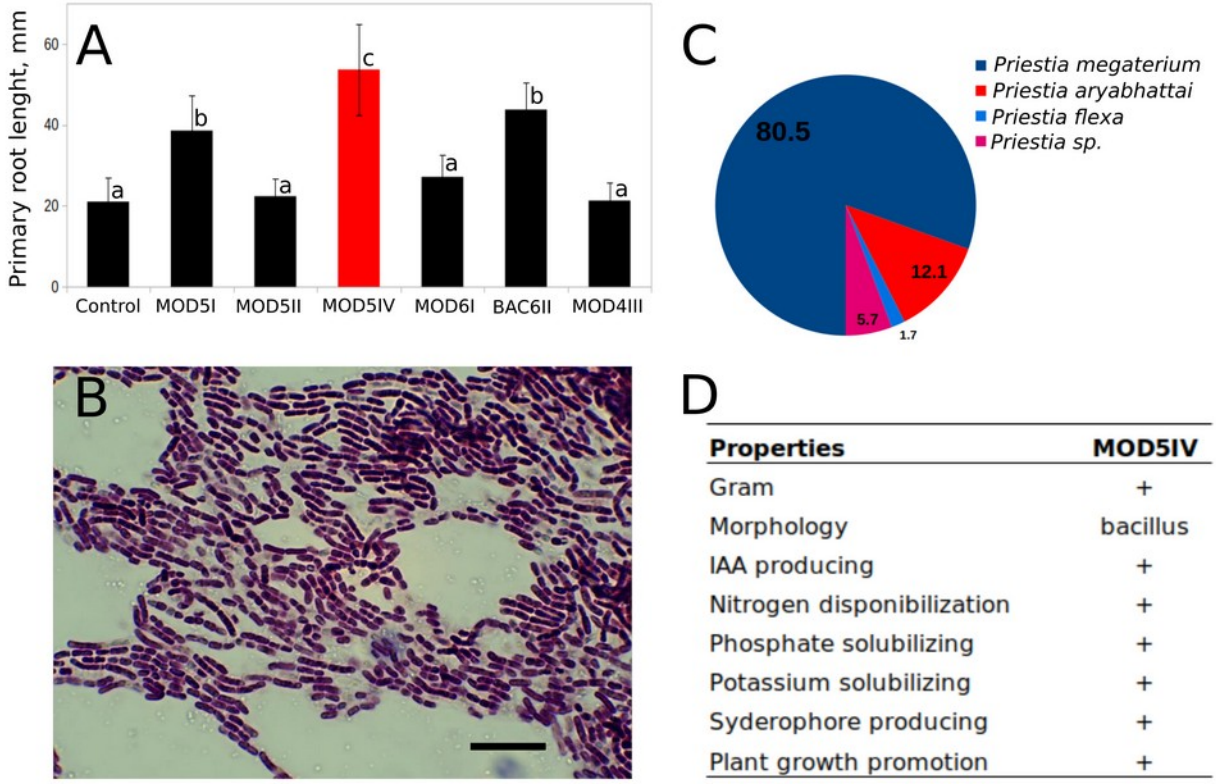

Properties	MOD5IV
Gram	+
Morphology	bacillus
IAA producing	+
Nitrogen disponibilization	+
Phosphate solubilizing	+
Potassium solubilizing	+
Syderophore producing	+
Plant growth promotion	+

Figure 1. Selection of Isolates, Plant Growth Promotion Capacity, and General Characterization of Strain MOD5IV. (A) *Arabidopsis thaliana* primary root growth promotion by the isolated strains. The red column represents the strain MOD5IV, which had the highest plant growth promotion capacity. a, b and c indicate significant differences estimated using Two-way ANOVA ($p < 0.05$). Parametricity was estimated using the Kolmogorov-Smirnov Test of Normality. N = 9 (B) MOD5IV morphology as revealed by bright-field microscopy and Gram staining (scale bar indicates 25 µm). (C) Species distribution map of MOD5IV 16S rDNA compared to the NR database (numbers represent the percentage of representation of the 100 best hits in BLAST analysis). (D) Summary of the morphological characteristics and plant growth promotion properties of strain MOD5IV.

Figure 2

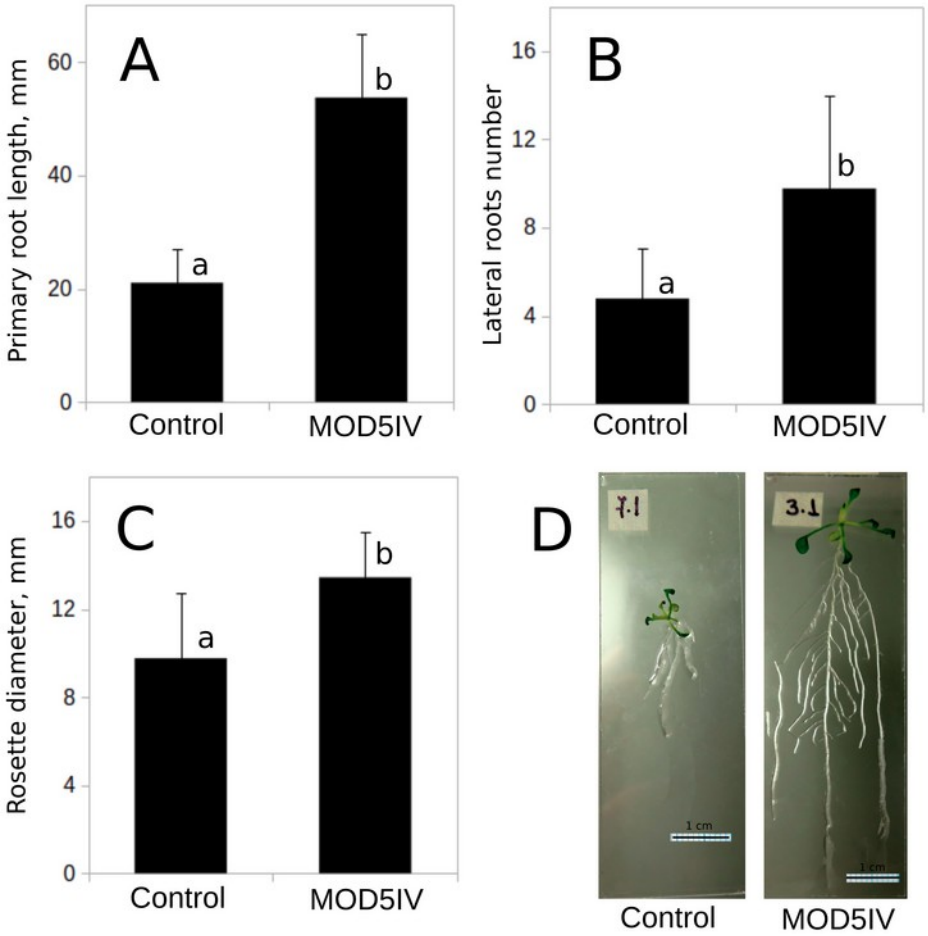

Figure 2. *P. megaterium* MOD5IV Promotes *Arabidopsis thaliana* Growth In Vitro. (A) Promotion of *A. thaliana* primary root growth by the MOD5IV strain. **(B)** Promotion of *A. thaliana* lateral root development induced by the MOD5IV strain. **(C)** Growth of *A. thaliana* rosette induced by MOD5IV. a and b indicate significant differences estimated by Two-way ANOVA $p < 0.05$. Parametricity was estimated by Kolmogorov-Smirnov Test of Normality. N = 9 **(D)** Representative images of *A. thaliana* plants exposed to MOD5IV and not exposed (Control) in a 15-day co-culture experiment.

Table 1

Table1. General genome features of *P. megaterium* MOD5IV compared with other five *Priestia* strains.

Strains	*P. megaterium* MOD5IV	*P. megaterium* NCT-2	*P. megaterium* DSM 319	*P. megaterium* KF18	*P. megaterium* NBRC 15308	*P. flexa* KLBMP 4941
Genome size (Mb)	5.7	5.9	5.1	6.0	5.7	4.1
Chromosome size (Mb)	5.3	5.2	5.1	5.2	5.3	3.96
G+C content (%)	37.7	37.8	38.1	37.6	38.0	38.0
Chromosomal G+C content (%)	38.0	38.2	38.1	38.1	38.0	38.1
Gene number	6,211	6,134	5,337	6,294	6,003	4,332
Coding sequence number	6,022	5,805	4,994	5,979	5,754	3,971
RNA gene number	189	203	153	217	163	143
rRNA genes	46	53	33	46	41	36
tRNA gene number	143	142	114	163	122	102
Plasmid number	9	10	0	9	6	2

Figure 3

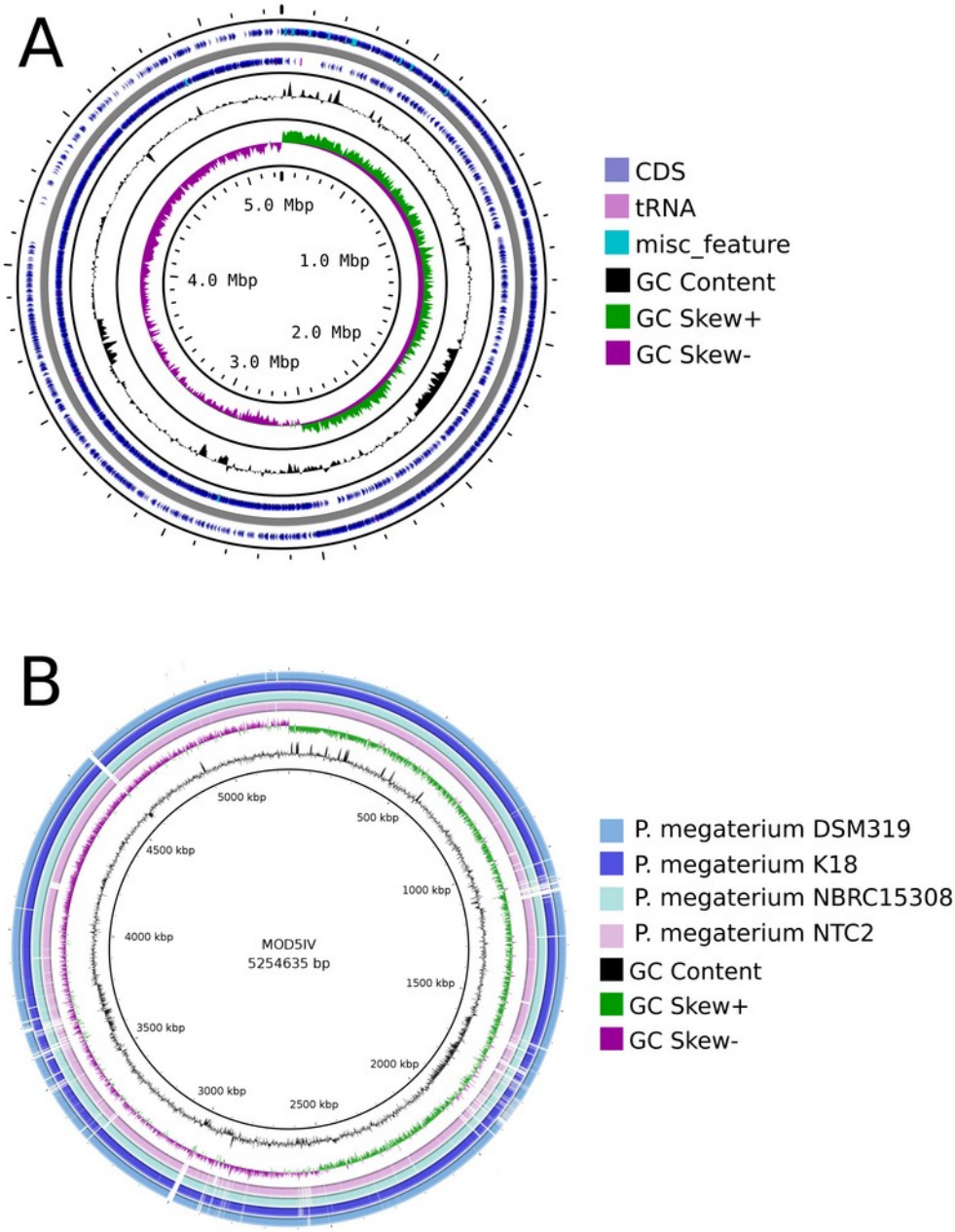

Figure 3. Genome map of *P. megaterium* MOD5IV and comparison with other *P. megaterium* genomes. A) Chromosome map prepared using Proksee software. Circles from outside to inside show the position of protein-coding sequences (blue), tRNA genes (pink), and rRNA genes (cyan) on the positive (circle 1) and negative (circle 2) strands. Circles 3 and 4 show plots of GC content and GC skew as deviations from the average for the entire sequence. B) BRIG output image. The draft of the *P. megaterium* MOD5IV genome aligned against other *P. megaterium* genomes (DM319, K18, NBRC15305 = ATCC 14581, NTC2). GC content and skew are also shown.

Figure 4

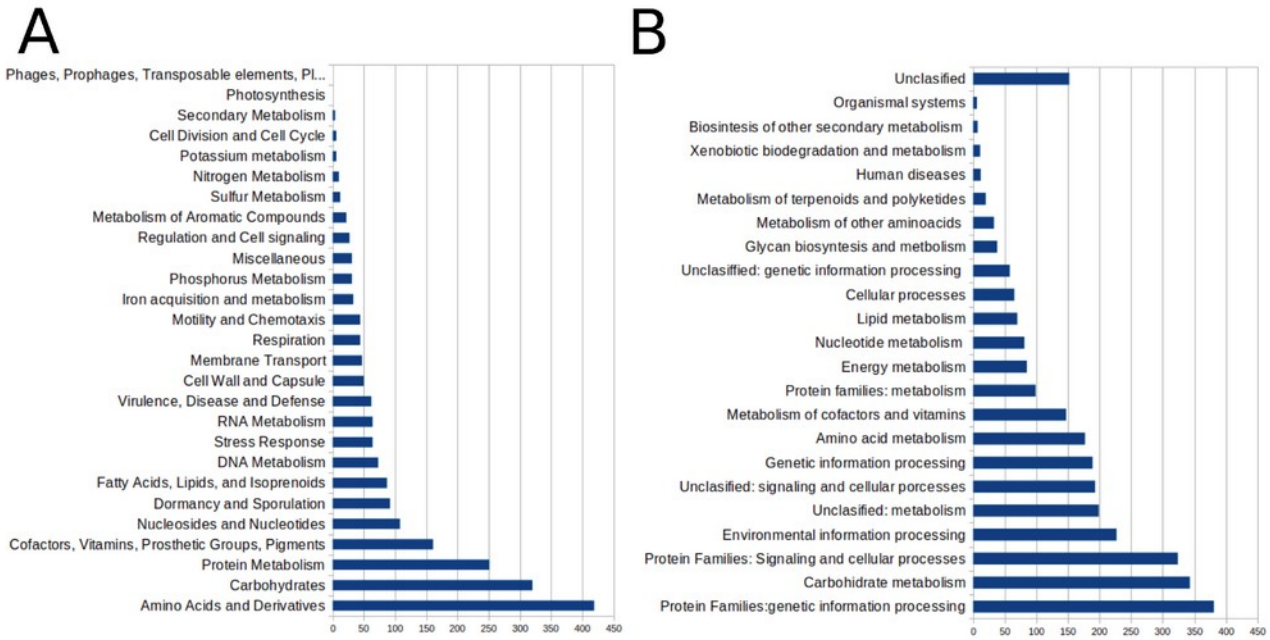

Figure 4. Predicted functions encoded in the *P. megaterium* MOD5IV genome. A) Statistical chart of the RAST subsystem category distribution. The y-axis represents the classification of different functional genes in the RAST subsystem classification. B) Statistical chart of the KEGG annotation classes. The y-axis represents the classification of different functional genes in the KEGG database.

Figure 5

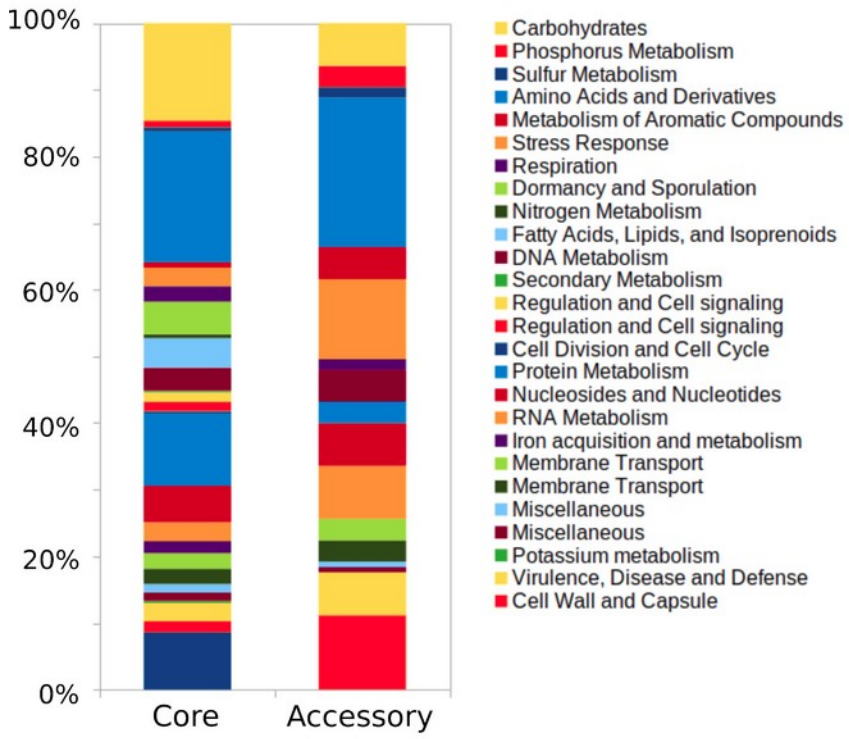

Figure 5. MOD5IV Accessory Genome Analysis. RAST subsystem classification of the MOD5IV core and accessory genome determined by Spine/AGEnt. Data is presented as a percentage of the total genes in the core and accessory genome.

Table 2

Table 2. General features of the chromosome and plasmids present in *P. megaterium* MOD5IV genome.

	Chromosome	pMOD5IV 1	pMOD5IV 2	pMOD5IV 3	pMOD5IV 4	pMOD5IV 5	pMOD5IV 6	pMOD5IV 7	pMOD5IV 8	pMOD5IV 9
Size (pb)	5,254,635	125.337	112.536	69.915	47.78	42.938	10.013	9.405	8.643	8.518
GC Content	38.0	34.1	34.5	31.7	32.0	37.3	34.8	34.4	33.8	34.5
Number of RAST Subsystems	334	9	6	6	0	0	0	0	0	1
Number of Coding Sequences	5,554	140	62	84	53	42	14	10	13	11
Number of RNAs	168	0	0	0	0	20	0	0	0	0

Table 3.

Table 3. Summary of Gene Functions Related to Plant Growth Promotion and Resistance to Metals and Metalloids in the *P. megaterium* MOD5IV Genome.

	Gene function
N.°	**Fe metabolism and uptake**
1	Sdab Siderophore biosynthesis diaminobutyrate--2-oxoglutarate aminotransferase
2	Sdab Siderophore biosynthesis L-2,4-diaminobutyrate decarboxylase
3	SSIAc Siderophore synthetase large component, acetyltransferase.
4	SssAc Siderophore synthetase small component, acetyltransferase.
5	SSLc Siderophore synthetase component, ligase.
6	SbsM Siderophore biosynthesis protein, monooxygenase.
7	Stra Siderophore transport protein
8	ABCp ABC-type Fe3+-siderophore transport system, permease component
9	ABCatp ABC-type Fe3+-siderophore transport system, ATPase component
10	ABCsb ABC-type Fe3+-siderophore transport system, periplasmic iron-binding component.
11	ABCp2 ABC-type Fe3+-siderophore transport system, permease 2 component.
12	X-ABC3 ABC Uncharacterized iron compound ABC uptake transporter, ATP-binding protein
13	Fe-ABC1 Iron compound ABC uptake transporter substrate-binding protein
14	Fe-ABC2 Iron compound ABC uptake transporter permease protein
15	HtsABC Heme ABC type transporter HtsABC, heme-binding protein.
16	HrtAB Sensor histidine kinase colocalized with HrtAB transporter.
17	X-ABC Uncharacterized iron compound ABC uptake transporter, ATP-binding protein.
18	Iron compound ABC uptake transporter permease protein
19	ZnH Zn-dependent hydrolase YycJ/WalJ
20	Two-component response regulator SA14-24
21	Two-component sensor kinase SA14-24
N.°	**Phosphate metabolism and uptake**
1	PhoU Phosphate transport system regulatory protein.
2	PhoP Alkaline phosphatase synthesis transcriptional regulatory protein.
3	PhoR Phosphate regulon sensor protein (SphS)
4	PhoB Phosphate regulon transcriptional regulatory protein (SphR)
5	Polyphosphate kinase
6	Manganese-dependent inorganic pyrophosphatase
7	PhoH Predicted ATPase related to phosphate starvation-inducible protein
8	Alkaline phosphatase
9	Probable low-affinity inorganic phosphate transporter
10	Exopolyphosphatase
N.°	**Potassium metabolism and uptake**
1	Large-conductance mechanosensitive channel.
2	Potassium efflux system KefA protein
N.°	**Auxin biosyntesis**
1	Anthranilate phosphoribosyltransferase
2	Phosphoribosylanthranilate isomerase
3	Tryptophan synthase alpha chain
4	Tryptophan synthase beta chain
5	Amino transferase
6	Indolepyruvate decarboxylase
7	IAAld dehydrogenase
8	Trp decarboxylase
9	Tryptophan acetyltransferase
10	Nitrilase
N.°	**Nitrogen metabolism and uptake**
1	NsrR Nitrite-sensitive transcriptional repressor
2	Glutamine synthetase type I
3	Glutamate synthase [NADPH] small chain
4	Ferredoxin-dependent glutamate synthase
5	Nitrogen regulatory protein P-II
6	Ammonium transporter
7	Assimilatory nitrate reductase large subunit
8	Nitrite reductase [NAD(P)H] large subunit
9	Nitrate/nitrite transporter NarT
10	NorD, Nitric oxide reductase activation protein
11	NorQ, Nitric oxide reductase activation protein
12	Oxygen-insensitive NAD(P)H nitroreductase
N.°	**Metal resistance**
1	MerR Transcriptional regulator, MerR family.
2	ArsR Arsenical resistance operon repressor
3	ArsC Arsenate reductase (EC 1.20.4.4) thioredoxin-coupled, LMWP family
4	Arsenite/antimonite:H+ antiporter ArsB
5	ArsR Arsenical resistance operon repressor
6	ArsB Arsenite/antimonite:H+ antiporter
7	Lead, cadmium, zinc and mercury transporting ATPase (EC 3.6.3.3) (EC 3.6.3.5)
8	Multidrug resistance transporter, Bcr/CflA family
9	Copper resistance protein CopC
10	Copper resistance protein CopD
11	Cobalt-zinc-cadmium resistance protein
12	Cadmium-transporting ATPase
13	Response regulator of zinc sigma-54-dependent two-component system
14	Cytoplasmic copper homeostasis protein CutC
15	CadA Cadmium-transporting ATPase (EC 3.6.3.3)
16	CadC Cadmium efflux system accessory protein

Figure 6

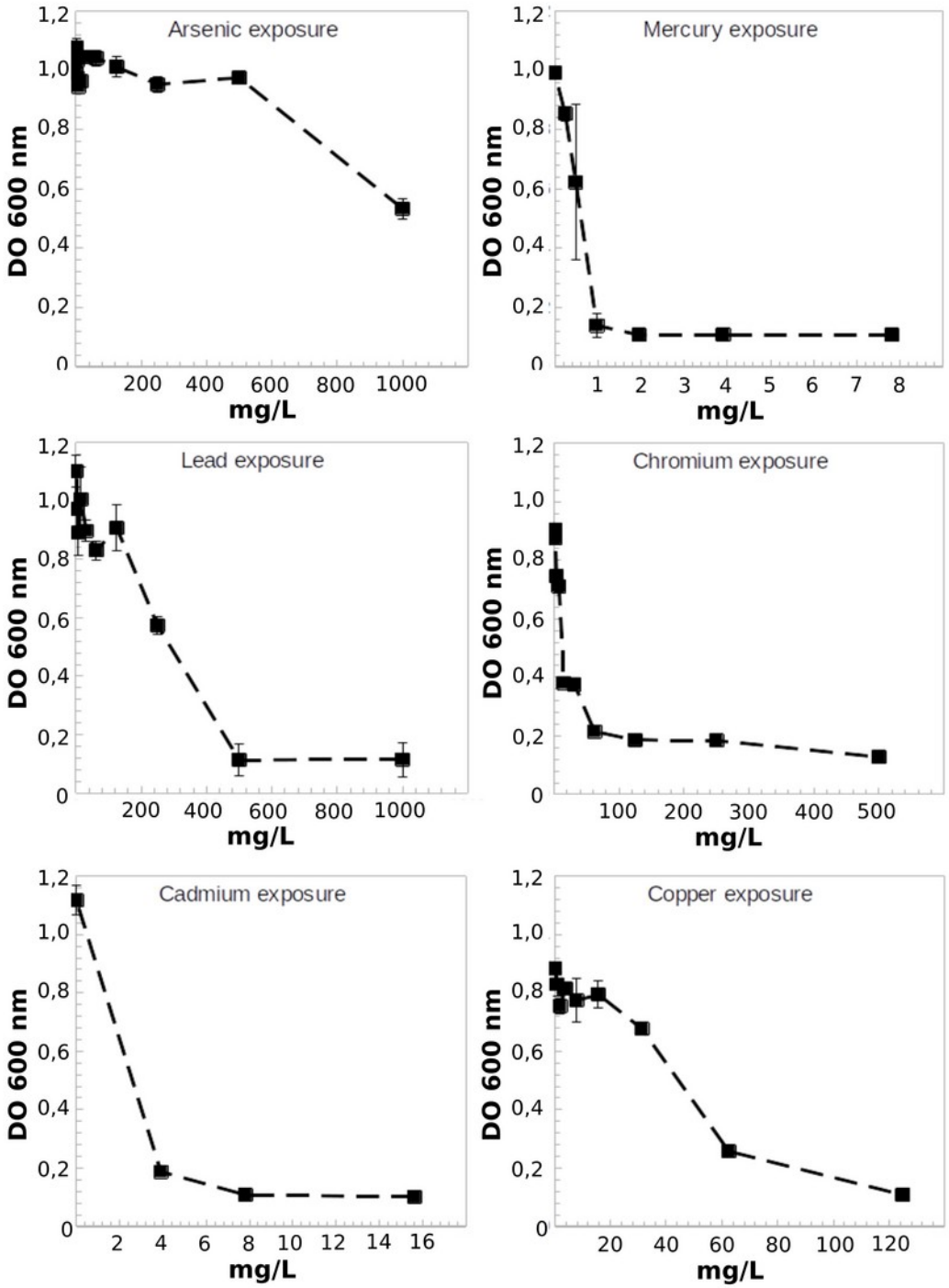

Figure 6. *P. megaterium* MOD5IV Metal Resistance. Maximum growth of MOD5IV in TSB medium supplemented with increasing concentrations of metals (as indicated in each figure), measured by absorbance at 600 nm. Error bars indicate the standard deviation of average of three independent experiments.

Figure 7

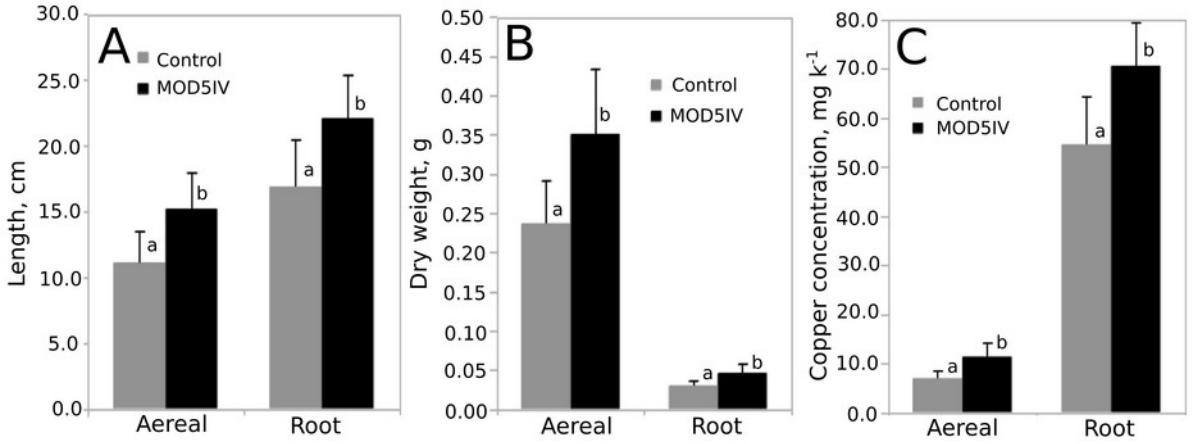

Figure 7. *P. megaterium* MOD5IV Increases Growth and Copper Uptake in *Caesalpinia spinosa*. Two-month-old *C. spinosa* plants were grown in mine tailings amended with organic substrate, with or without inoculation with *P. megaterium* MOD5IV. (A) aerial (shoot + leafs) and root length of *C. spinosa*. (B) Dry weight of *C. spinosa* aerial organs and roots. (C) Copper accumulation in aerial organs and roots of *C. spinosa*. a and b indicate significant differences estimated using Two-way ANOVA ($p < 0.05$). Parametricity was estimated by the Kolmogorov-Smirnov Test of Normality.

Bibliography

1 Abdelkrim, S., Jebara, S.H., Saadani, O. Chiboub, M., Abid, G., Mannai, K. & Jebara M. Heavy metal accumulation in *Lathyrus sativus* growing in contaminated soils and identification of symbiotic resistant bacteria. *Arch Microbiol* 201, 107–121 (2019). https://doi.org/10.1007/s00203-018-1581-4

2 Adeniji, A., Chukwuneme, C., Conceição, E., Ayangbenro A., Wilkinson E. Maasdorp, E, de Oliveira, T. and Babalola, O. (2025). Unveiling novel features and phylogenomic assessment of indigenous *Priestia megaterium* AB-S79 using comparative genomics. Microbiology Spectrum.

3 Alcock, B. P., Raphenya, A. R., Lau, T. T. Y., Tsang, K. K., Bouchard, M., Edalatmand, A., ... & McArthur, A. G. (2023). CARD 2023: Expanded Curation, Support for Machine Learning, and Resistome Prediction at the Comprehensive Antibiotic Resistance Database. *Nucleic Acids Research, 51*, D690-D699. https://doi.org/10.1093/nar/gkac920

4 Alcock, B. P., Raphenya, A. R., Lau, T. T. Y., Tsang, K. K., Bouchard, M., Edalatmand, A., ... & McArthur, A. G. (2020). CARD 2020: Antibiotic resistome surveillance with the comprehensive antibiotic resistance database. *Nucleic Acids Research, 48*(D1), D517-D525. https://doi.org/10.1093/nar/gkz935

5 Alexander, D. B. & Zuberer, D. A. (1991). Use of chrome azurol S reagents to evaluate siderophore production by rhizosphere bacteria. Biology and Fertility of Soils, 12(1): 39– 45. https://doi.org/10.1007/BF00369386

6 Alikhan, N. F., Petty, N. K., Ben Zakour, N. L., & Beatson, S. A. (2011). BLAST Ring Image Generator (BRIG): simple prokaryote genome comparisons. *BMC Genomics, 12*, 402. https://doi.org/10.1186/1471-2164-12-402

7 Alves, L. S., Yin Q., Oliveira R.S., Silva, E.F., & Novo, L.A.B. (2022). Plant growth-promoting bacteria in phytoremediation of metal-polluted soils: Current knowledge and future directions. *Science of the Total Environment, 838*, 156435. http://dx.doi.org/10.1016/j.scitotenv.2022.156435

8 Andrews, S. (2010). FastQC: A Quality Control Tool for High Throughput Sequence Data. Retrieved from http://www.bioinformatics.babraham.ac.uk/projects/fastqc

9 Ashraf, S., Ali, O., Zahir, Z.A., Ashraf, S. & Asghar, H.N. (2019). Assessment of phytoremediation potential of native plants growing on Pb mine waste. *Ecotoxicology and Environmental Safety, 174*, 714-727. https://doi.org/10.1016/j.ecoenv.2019.02.068

10 Asad, S. A., Farooq, M., Afzal, A., & West H (2018). Integrated phytobial heavy metals remediation strategies for sustainable clean environment - A review . *Chemosphere, 217*, 925-941. http://dx.doi.org/10.1016/j.chemosphere.2018.11.021

11 ASTM International, 2018. Standard Practice for Reducing Samples of Aggregate to Testing Size, C702/C702M- 18. West Conshohocken, PA.

12 Astorga-Eló, M., Gonzalez, S., Acuña, J.J., Sadowsky, M.J., Jorquera, M.A. (2021). Rhizobacteria from 'flowering desert' events contribute to the mitigation of water scarcity stress during tomato seedling germination and growth. Sci Rep., 11(1):13745. https://doi: 10.1038/s41598-021-93303-8.

13 Azhar, U., Ahmad, H., Shafqat, H., Babar, M., Munir H. M. S., Sagir, M., Arif, M., Hassan, A., Rachmadona, N., Rajendran, S., Mubashir, M. & Khoo, K. S. (2022). Remediation techniques for elimination of heavy metal pollutants from soil: A review. *Environmental Research, 214*, 113918. https://doi.org/10.1016/j.envres.2022.113918

14 Bhatt, K. & Maheshwari, D.K. (2020) Zinc solubilizing bacteria (*Bacillus megaterium*) with multifarious plant growth promoting activities alleviates growth in *Capsicum annuum* L. *3 Biotech* 10, 36. https://doi.org/10.1007/s13205-019-2033-9

15 Backer, R., Rokem, J. S., Ilangumaran, G., Lamont, J., Praslickova, D., Ricci, E., Subramanian, S., & Smith, D. L. (2018). Plant growth-promoting rhizobacteria: Context, mechanisms of action, and roadmap to commercialization of biostimulants for sustainable agriculture. *Frontiers in Plant Science, 9*, 1473. https://doi.org/10.3389/fpls.2018.01473

16 Becking, J.H. (2006). The Family Azotobacteraceae. In: Dworkin, M., Falkow, S., Rosenberg, E., Schleifer, KH., Stackebrandt, E. (eds) The Prokaryotes. Springer, New York, NY. https://doi.org/10.1007/0-387-30746-X_26

17 Castro-Severyn, J., Fortt, J., Sierralta, M., Alegria, P., Donoso, G., Choque, A., Avellaneda, A.M., Pardo-Esté, C., Saavedra, C.P., Stoll, A., Remonsellez, F. (2024). Rhizospheric bacteria from the Atacama Desert hyper-arid core: cultured community dynamics and plant growth promotion. Microbiol Spectr., 12(6):e0005624. https://doi: 10.1128/spectrum.00056-24.

18 Chakraborty, U., Chakraborty, B. & Basnet, M. (2006). Heavy metal resistance in microorganisms: Physiology and molecular mechanisms. *Journal of Basic Microbiology, 46(3)*, 186-195. https://doi.org/10.1002/jobm.200510050

19 Cui, Z., Hu, L., Zeng, L., Meng, W., Guo, D. & Sun, L. (2023). Isolation and characterization of *Priestia megaterium* KD7 for the biological control of pear fire blight. Front Microbiol. 14, 1099664. https://doi.org/10.3389/fmicb.2023.1099664

20 Efe, D. (2020) Potential Plant Growth-Promoting Bacteria with Heavy Metal Resistance. *Curr Microbiol* **77**, 3861–3868 . https://doi.org/10.1007/s00284-020-02208-8

21 Gao, Y., Miao, C., Mao, L., Zhou, P., Jin, Z. & Shi, W. (2010). Improvement of phytoextraction and antioxidative defense in *Solanum nigrum* L. under cadmium stress by application of cadmium-resistant strain and citric acid. Journal of Hazardous Materials 181, 771–777. https://doi.org/10.1016/j.jhazmat.2010.05.080

22 Glick, B. R. (2012). Plant Growth-Promoting Bacteria: Mechanisms and Applications. *Scientifica, 2012, 963401*. http://dx.doi.org/10.6064/2012/963401

23 Glickmann, E. & Dessaux, Y. (1995). A critical examination of the specificity of the Salkowski reagent for indolic compounds produced by phytopathogenic bacteria. Appl Environ Microbiol. 61(2), 793-796. https://doi.org/10.1128/aem.61.2.793-796.1995

24 Guardado-Fierros, B., Tuesta-Popolizio, D., Lorenzo-Santiago, M., Rodriguez-Campos, J. and Contreras-Ramos, S. (2024). Comparative study between Salkowski reagent and chromatographic method for auxins quantification from bacterial production. Front. Plant Sci. 15 – 2024. https://doi.org/10.3389/fpls.2024.1378079

25 Guzmán-Moreno, J., García-Ortega, L.F., Torres-Saucedo, L., Rivas-Noriega, P., Ramírez-Santoyo, R.M., Sánchez-Calderón, L., Quiroz-Serrano, L.N.& Vidales-Rodríguez, L.E. 2022. *Bacillus megaterium* HgT21: a Promising Metal Multiresistant Plant Growth-Promoting Bacteria for Soil Biorestoration. Microbiol Spectr 10:e00656-22. https://doi.org/10.1128/spectrum.00656-22

26 Hernández-Soberano, C., Ruíz-Herrera, L.F. & Valencia-Cantero E (2020). Endophytic bacteria *Arthrobacter agilis* UMCV2 and *Bacillus methylotrophicus* M4-96 stimulate achene germination, in vitro growth, and greenhouse yield of strawberry (*Fragaria* × *ananassa*) *Scientia Horticulturae, 261*, 109005. https://doi.org/10.1016/j.scienta.2019.109005

27 Jacob J.M., Karthik, C., Saratale R.G., Kumar S.S., Prabakar, D., Kadirvelu K. & Pugazhendhi A. (2018). Biological approaches to tackle heavy metal pollution: A survey of literature . *Journal of Environmental Management, 217*, 56-70. https://doi.org/10.1016/j.jenvman.2018.03.077

28 Kamaruzzaman, M. A., Abdullah, S. R. S., Hasan, H. A., Hassan M., Othman, A.R. & Idris, M. (2020). Characterisation of Pb-resistant plant growth-promoting rhizobacteria (PGPR) from

Scirpus grossus. *Biocatalysis and Agricultural Biotechnology, 23*, 101456. http://dx.doi.org/10.1016/j.bcab.2019.101456

29 Khoshru, B., Mitra, D., Khoshmanzar, E., Myo, E. M., Uniyal, N., Mahakur, B. & Rani, A. (2020). Current scenario and future prospects of plant growth-promoting rhizobacteria: an economic valuable resource for the agriculture revival under stressful conditions. *Journal of Plant Nutrition*, *43*(20), 3062–3092. https://doi.org/10.1080/01904167.2020.1799004

30 Kong, Z., Mohamad, O.A., Deng, Z. *et al.* Rhizobial symbiosis effect on the growth, metal uptake, and antioxidant responses of *Medicago lupulina* under copper stress. *Environ Sci Pollut Res* **22**, 12479–12489 (2015). https://doi.org/10.1007/s11356-015-4530-7

31 latorre, M., Olivares, F., Reyes-Jara, A., López, G. & González, M. (2011). CutC is induced late during copper exposure and can modify intracellular copper content in *Enterococcus faecalis* Biochemical and Biophysical Research Communications, 406(4), 633-637 https://doi.org/10.1016/j.bbrc.2011.02.109

32 Lawton, T.J., Kenney, G.E., Hurley, J.D. & Rosenzweig A.C. (2016). The CopC Family: Structural and Bioinformatic Insights into a Diverse Group of Periplasmic Copper Binding Proteins. Biochemistry, 55 (15), 2278-2290. https://doi.org/10.1021/acs.biochem.6b00175

33 Liu, S., Wang, X., Guo, G. & Yan, Z. (2021) Status and environmental management of soil mercury pollution in China: A review. Journal of Environmental Management, 277, 111442. https://doi.org/10.1016/j.jenvman.2020.111442.

34 Liu A, Wang, W,, Zheng, X., Chen, X., Fu, W., Wang G., Ji, J., Jin, C., Guan C. (2022). Improvement of the Cd and Zn phytoremediation efficiency of rice (*Oryza sativa*) through the inoculation of a metal-resistant PGPR strain. *Chemosphere, 302*, 134900. https://doi.org/10.1016/j.chemosphere.2022.134900

35 Ma, Y., Prasad, M.N.V., Rajkumar, M., & Freitas, H. (2011). Plant growth promoting rhizobacteria and endophytes accelerate phytoremediation of metalliferous soils. *Biotechnology Advances, 29(2)*, 248-258. https://doi.org/10.1016/j.biotechadv.2010.12.001

36 Manoj, S.R., Karthik, C., Kadirvelu, K., Arulselvi P.I., Shanmugasundaram, T., Bruno, B. & Rajkumar, M (2020). Understanding the molecular mechanisms for the enhanced phytoremediation of heavy metals through plant growth promoting rhizobacteria: A review. *Journal of Environmental Management, 254*, 109779. https://doi.org/10.1016/j.jenvman.2019.109779

37 Maza, F., Maldonado, J., Vásquez-Dean, J., Mandakovic, D., Gaete, A., Cambiazo, V., González, M. (2019). Soil Bacterial Communities From the Chilean Andean Highlands:

Taxonomic Composition and Culturability. Front Bioeng Biotechnol.. 7:10. https://doi: 10.3389/fbioe.2019.00010.

38 Mengoni, A., Barzanti, R., Gonnelli, C., Gabbrielli, R. & Bazzicalupo, M. (2001) Characterization of nickel- resistant bacteria isolated from serpentine soil. Environmental Microbiology, 3(11), 691–698 https://doi.org/10.1046/j.1462-2920.2001.00243.x

39 Meier-Kolthoff, J.P., Carbasse, J.S., Peinado-Olarte R.L. & Göker M. (2022). TYGS and LPSN : a database tandem for fast and reliable genome-based classification and nomenclature of prokaryotes. Nucleic Acids Research, 50. 801-807. https://doi.org/10.1093/nar/gkab902

40 Myo, E.M., Ge, B., Ma, J. Cui, H., Liu, B.,, Shi, L., Jiang, M., & Zhang K. (2019) Indole-3-acetic acid production by *Streptomyces fradiae* NKZ-259 and its formulation to enhance plant growth. *BMC Microbiol* **19**, 155. https://doi.org/10.1186/s12866-019-1528-1

41 Naqqash, T., Imran, A., Hameed, S. Shahid, M., Majeed, A., Iqbal, J., Hanif, M.K., Ejaz, S. & Malik K.A. (2020) First report of diazotrophic *Brevundimonas* spp. as growth enhancer and root colonizer of potato. *Sci Rep* **10**, 12893 . https://doi.org/10.1038/s41598-020-69782-6

42 Nautiyal, C. S. (1999). An efficient microbiological growth medium for screening phosphate solubilizing microorganisms. FEMS Microbiology Letters, 170(1), 265-270. https://doi.org/10.1111/j.1574-6968.1999.tb13383.x

43 Nazari, M., & Smith, D. L. (2020). A PGPR-Produced Bacteriocin for Sustainable Agriculture: A Review of Thuricin 17 Characteristics and Applications. Frontiers in Plant Science, 1*1*, 916. https://doi.org/10.3389/fpls.2020.00916

44 Overbeek, R., Olson, R., Pusch, G. D., Olsen, G. J., Davis, J. J., Disz, T., & Stevens, R. (2014). The SEED and the Rapid Annotation of microbial genomes using Subsystems Technology (RAST). *Nucleic Acids Research, 42*, D206-D214. https://doi.org/10.1093/nar/gkt1226

45 Parviainen, A., Vázquez-Arias, A., Arrebola, J.P. & Martín-Peinado, F.J. (2022). Human health risks associated with urban soils in mining areas. *Environmental Research, 206*, 112514. https://doi.org/10.1016/j.envres.2021.112514

46 Rensing, C., & Grass, G. (2003). Escherichia coli mechanisms of copper homeostasis in a changing environment. *FEMS Microbiology Reviews, 27*(2-3), 197-213. https://doi.org/10.1016/S0168-6445(03)00049-4

47 Roane, T. M. (1999). Lead resistance in two bacterial isolates from heavy metal–contaminated soils. *Microb Ecol **37**, 218–224. https://doi.org/10.1007/s002489900145*

48 Romero-Estonllo, M., Ramos-Castro, J., San Miguel del Río, Y., Rodríguez-Garrido, B., Prieto-Fernández, Á., Kidd, P.S. & Monterroso, C. (2023). Soil amendment and rhizobacterial

inoculation improved Cu phytostabilization, plant growth and microbial activity in a bench-scale experiment. *Front. Microbiol*. 14, 1184070. https://doi.org/10.3389/fmicb.2023.1184070

49 Sánchez-Castro, I., Molina, L., Prieto-Fernández, M.A. & Segura A (2023). Past, present and future trends in the remediation of heavy-metal contaminated soil - Remediation techniques applied in real soil-contamination events. *Heliyon, 9 (6)*, e16692. https://doi.org/10.1016/j.heliyon.2023.e16692

50 Shao, J., Li, S., Zhang, N. Cui, X., Zhou, X., Zhang, G., Shen, Q., & Zhang R. (2015). Analysis and cloning of the synthetic pathway of the phytohormone indole-3-acetic acid in the plant-beneficial *Bacillus amyloliquefaciens* SQR9. Microb Cell Fact **14**, 130 (2015). https://doi.org/10.1186/s12934-015-0323-4

51 Sijilmassi, B., Filali-Maltouf, A., Boughribil, S., Kumar, S., & Amri, A. (2020). In-vitro plant growth promotion of *Rhizobium* strains isolated from lentil root nodules under abiotic stresses. *Agronomy, 10*(7), 1006. https://doi.org/10.3390/agronomy10071006

52 Simmer, R.A., & Schnoor, J. L. (2022). Phytoremediation, Bioaugmentation, and the Plant Microbiomes. *Environmental Science & Technology, 56(23)*, 2958-2970. https://doi.org/10.1021/acs.est.2c05970

53 Smaldone, G., & Helmann, J.D. (2007). CsoR regulates the copper efflux operon copZA in *Bacillus subtilis.* Microbiology, *153*, 4123-4128. https://doi.org/10.1099/mic.0.2007/011742-0

54 Souza, L.R.R., Pomarolli, L.C. & da Veiga, M.A.M.S. (2020) From classic methodologies to application of nanomaterials for soil remediation: an integrated view of methods for decontamination of toxic metal(oid)s. *Environ Sci Pollut Res*, 27, 10205–10227 . https://doi.org/10.1007/s11356-020-08032-8.

55 Shrestha, P., Kim, M., Elbasani, E., Kim, J-D and Oh, T-J. Prediction of trehalose-metabolic pathway and comparative analysis of KEGG, MetaCyc, and RAST databases based on complete genome of *Variovorax* sp. PAMC28711. BMC Genomic Data. 234. https://doi.org/10.1186/s12863-021-01020-y.

56 Srinath, T., Verma, T., & Ramteke, P. W. (2002). Chromium(VI) biosorption and bioaccumulation by chromate resistant bacteria. *Chemosphere*, *48*, 427-435. https://doi.org/10.1016/s0045-6535(02)00089-9.

57 Srivastava, S., Verma, P.C., Chaudhry, V., Singh, N., Abhilash, P.C., Kumar, K.V. Sharma, N. & Singh, N. (2013). Influence of inoculation of arsenic-resistant *Staphylococcus arlettae* on growth and arsenic uptake in *Brassica juncea* (L.) Czern. Var. R-46. *Journal of Hazardous Materials, 262*, 1039-1047. https://doi.org/10.1016/j.jhazmat.2012.08.019

58 Stothard, P., & Wishart, D. S. (2005). Circular genome visualization and exploration using CGView. *Bioinformatics, 21*(4), 537–539. https://doi.org/10.1093/bioinformatics/bti054

59 Tang, L., Hamid, Y., Zehra, A., Sahito, Z.A., He, Z., Beri, W.T. Khan, M.B. & Yang, X (2020). Fava bean intercropping with *Sedum alfredii* inoculated with endophytes enhances phytoremediation of cadmium and lead co-contaminated field. *Environmental Pollution, 265*, 114861. https://doi.org/10.1016/j.envpol.2020.114861

60 Tien, T. M., Gaskins, M. H., & Hubbell, D. H. (1979). Plant growth substances produced by *Azospirillum brasilense* and their effect on the growth of Pearl millet (*Pennisetum americanum* L.). Applied and Environmental Microbiology, *37(5)*, 1016-1024. https://doi.org/10.1128/aem.37.5.1016-1024.1979

61 Tirry, N., Kouchou, A., El Omari, B., Ferioun, M. & El Ghachtouli, N. (2021). Improved chromium tolerance of *Medicago sativa* by plant growth-promoting rhizobacteria (PGPR). *Journal of Genetic Engineering and Biotechnology, 19(1), 149*. https://doi.org/10.1186/s43141-021-00254-8

62 Ullah, A., Heng, S., & Munis, M. F. H., Fahad, S. & Yang, X. (2022). Phytoremediation of heavy metals assisted by plant growth promoting (PGP) bacteria: A review. *Environmental and Experimental Botany, 117*, 28-40. https://doi.org/10.1016/j.envexpbot.2015.05.001

63 Ustiatik, R., Nuraini, Y., Suharjono, S., Jeyakumar, P., Anderson, C. W. N., & Handayanto, E. (2021). Mercury resistance and plant growth promoting traits of endophytic bacteria isolated from mercury-contaminated soil. *Bioremediation Journal*, *26*(3), 208–227. https://doi.org/10.1080/10889868.2021.1973950

64 Wang, B., Zhang, D., Chu, S., Zhi, Y., Liu, X. & Zhou, P. (2020) Genomic Analysis of *Bacillus megaterium* NCT-2 Reveals Its Genetic Basis for the Bioremediation of Secondary Salinization Soil, International Journal of Genomics, 2020, 4109186 https://doi.org/10.1155/2020/4109186

65 Watanabe, F. S., & Olsen, S. R. (1965). Test of an ascorbic acid method for determining phosphorus in water and NaHCO3 extracts from soils. *Soil Science Society of America Journal, 29*, 677-678. http://dx.doi.org/10.2136/sssaj1965.03615995002900060025x

66 Wick, R. R., Judd, L. M., Gorrie, C. L., & Holt, K. E. (2017). Unicycler: Resolving bacterial genome assemblies from short and long sequencing reads. PLOS Computational Biology, 13(6), e1005595. . https://doi.org/10.1371/journal.pcbi.1005595

67 Wu, J., Kamal, N., Hao, H., Qian, C., Liu. Z., Shao, Y., Zhong, X. & Xu, B. (2019). Endophytic *Bacillus megaterium* BM18-2 mutated for cadmium accumulation and improving plant growth

in Hybrid *Pennisetum*. *Biotechnology Reports*, *23*, e00374. https://doi.org/10.1016/j.btre.2019.e00374

68 Wu, X., Zhao, Z., Zhao, Z., Zhang, Y., Li, M., & Yu, Q. (2023). Analysis of the Potassium-Solubilizing *Priestia megaterium* Strain NK851 and Its Potassium Feldspar-Binding Proteins. International Journal of Molecular Sciences, 24(18), 14226. https://doi.org/10.3390/ijms241814226

69 Xu, X., Xu, M., Zhao, Q. Zhang, Y., Li, M. & Yu, O. (2018) Complete Genome Sequence of Cd(II)-Resistant *Arthrobacter* sp. PGP41, a Plant Growth-Promoting Bacterium with Potential in Microbe-Assisted Phytoremediation. Curr Microbiol **75**, 1231–1239. https://doi.org/10.1007/s00284-018-1515-z

70 Zhou, C., Ma, Z., Zhu, L., Xiao, X., Xie, Y., Zhu, J. & Wang J. (2016). Rhizobacterial Strain *Bacillus megaterium* BOFC15 Induces Cellular Polyamine Changes that Improve Plant Growth and Drought Resistance. Int J Mol Sci., 17(6), 976. https://doi.org/10.3390/ijms17060976.